

# DOCUMENTATION OF HERITAGE SITES USING SURFACE TOPOGRAPHY AS CONTROL

Shahaf Levin, Sagi Filin

Transportation and Geo-Information Eng., Technion – Israel Institute of Technology, Haifa 32000, Israel - shahaf, filin@technion.ac.il

Commission V, WG V/2

**KEY WORDS:** Close Range Photogrammetry, Surfaces, Modeling

## ABSTRACT:

We present in this paper a model for the alignment of image sets using topographic data as control information. Traditional photogrammetric practices are based on points as control entities. These points have to be well measured and clearly marked within the scene. Additionally, for repeated measurement their demarcation should also be durable. Nonetheless, oftentimes the placement of photogrammetric control points cannot be readily implemented within the area for documentation. In many of those cases some form of topographic model, either coarse or fine, exists or can be readily established. This topographic description provides a broad and markerless coverage of control information, which if modeled appropriately, can substitute the use of control point network in the alignment process. While works on triangulation of aerial images to terrain models have been reported, close range applications offer challenges that are not common to the aerial case. We present in this paper a registration model for terrestrial images based on surfaces as control information. The paper addresses both the problem of acquiring mutual corresponding entities and the registration based on varying resolutions. The proposed model is applied for the mapping of prehistoric cave in the Carmel mountain ridge in Israel. Results show both the applicability of such model and that the estimation is comparable in quality to point based observations can be achieved.

## 1. INTRODUCTION

The application of terrestrial photogrammetry for documentation, modeling and reconstruction of cultural heritage sites is well established. This is due to the ease of data collection, availability of imaging devices, ability to avoid coming into physical contact with the mapped objects, and the well-established photogrammetric methodologies for the documentation.

Reviewing the body of works that have been devoted to photogrammetric reconstruction of heritage sites shows the use of image information in various levels of scale. As an example, Eisenbeiss et al. (2005) use radio-operated helicopter to acquire images for 3D modeling of the prehistoric site of Pinchango Alto in Peru. Lazaridou and Patmios (2005) describe the documentation of the Zagori region, a cultural heritage site located in the mountainous region in North-Western Greece. The authors make use of aerial and spaceborne imagery for that purpose. On a smaller scale and aiming for documentation of finer details, Kulur and Yilmaztürk (2005) use close-range photogrammetry and structured light for the 3D visualization of small historical objects for the Virtual Museum. Lerma et al. (2005) use close-range photogrammetry, advance image processing methods, and principle components analysis for 3D mapping of the Palaeolithic rock art motifs of Meravelles Cave (Valencia, Spain). A large scale project mixing technologies and models is reported in El-Hakim et al. (2007) who describe the 3D modeling of castles with use of a variety of surveying technologies including oblique and terrestrial photogrammetry, laser scanning, traditional electronic distance measurement (EDM), and additional architectural floor plans of the site.

A common thread to all the reported projects is the use of a dense control-point network for image geo-referencing.

However, the establishment of such network is not always a viable option. Marking points in sites for visual recognition, especially if multiple surveys are planned, can lead to site destruction and may not always be an option. Additionally, complex sites that call for dense control network will introduce difficulty in deploying sufficient control targets that can be well marked and durable within the site. This suggests that point based solutions cannot always be considered an option. Turning away from the classical point based solutions, and searching for natural control entities, a growing number of works have been proposing using linear features as control entities (e.g., van den Huvel, 1999; Zalmanson, 2000; Habib et al., 2003; Schenk, 2004). Nonetheless, lines, as points are hard to be found in open, unstructured regions.

The realization that a description of the surface topography exists in many sites in some level of resolution, means that object-space in its surficial form can be harnessed for the registration. Such scheme has the advantage of making use of available data without further requirements and allows for a markerless registration. The application of surface based photogrammetry has been proposed in the past, but for aerial cases. Ebner and Strunz (1988) introduced the concept of surface-based photogrammetry, motivating their choice by growing availability of Digital Terrain Models (DTMs) that can be employed as control information for certain photogrammetric applications. An expanded bundle-adjustment framework, which complements the fundamental collinearity equations with DTM-derived observation equations for the  $z$  ordinate of the estimated points, is proposed there. Jaw (2000) presents a similar approach using triangular-irregular-network (TIN) as control data. Ebner and Ohloh (1994) present an alternative approach utilizing surface information within the bundle block adjustment framework. The authors incorporate 3D ground control-points and local planar surfaces defined by unknown

surface points surrounding the control points. This model aims at utilizing ground control for photogrammetric block adjustment without point identification in image space. It is assumed that all control points lie on the terrain surface. Thus, they must lie on the plane defined by its surrounding points (at least three points are necessary).

The differences between aerial and terrestrial models, both in application and implementation, do not allow an immediate transfer of concepts/methodologies to the terrestrial problem. Three main aspects differentiate terrestrial models from the aerial ones. These include, i) overcoming the inherent occlusions associated with terrestrial imaging, ii) managing the different scales and resolution; and iii) finding correspondence between the photogrammetric and control information. In regards to occlusion, the natural surface topography leads to only partial information being visible in close-range models and thus leading to the "photogrammetric" interpreted surface to differ from the control one. In terms of scale and resolution, the density of the data in both surfaces varies greatly and leads to matching under different (and largely unknown) levels of detail between both sets. Finally, the establishment of correspondence requires a different approach than the standard aerial based solutions. Contrary to aerial photogrammetry where good approximated knowledge about the image pose parameters exists and allows establishing correspondence, the terrestrial case cannot enjoy such limiting assumptions. It requires answering how photogrammetric information and surface information should be used to define such parameters.

We present in this paper a surface based model for image georeferencing and its consequent application for site documentation from close-range images. The proposed model benefits from the use of the entire object-space and requires no marked points. The application of proposed model is applied to a documentation project of a prehistoric cave floor and the findings there. Difficult access to the cave ruled out the ability to use laser scanning for the documentation. The need to document the site through several repeated visits and the inability to mark fixed control points on the ground, made the formation of steady control network impossible. We, therefore, use a coarse surface model that was created in one visit as our control set. As we show, the level of accuracy in the image alignment was comparable to a point based solutions. This shows that photogrammetric procedures can be employed without the need for designated well-defined control targets.

## 2. SURFACE BASED PHOTOGRAMMETRY MODEL

The objectives of the proposed model are to develop a method for estimating the 3D pose parameters of terrestrial photogrammetric blocks with respect to a reference coordinate system, based on surface-models. Establishing a surface based model has the advantages of eliminating the need to identify corresponding control features in model and object space, and utilizing the entire object-space as control-entity (see Figure 1 Figure 1 that illustrates the concept). The sought model has to handle occlusions, manage the different scales and resolution, and for practical implementation provide a solution to the correspondence between both sets.

In order to overcome occlusions and the effects of scale changes within the images, the photogrammetric data is best represented as a pointset and the reference data as a surface model. Surface-based photogrammetry cannot provide single-photo solutions (contrary to point and line based methods), and require at least

two images. This suggests that the photogrammetric solution has to have some notion of 3D to 3D relation. Such relation translates into the registration of 3D datasets, which in photogrammetry relates to an absolute orientation problem.

The need to determine 3D coordinates in model-space necessitates the extraction of homologous point from the images. Taking advantage of the entire object-space as control entity requires a dense photogrammetric dataset, therefore an autonomous methods for the extraction of homologous points are desirable.

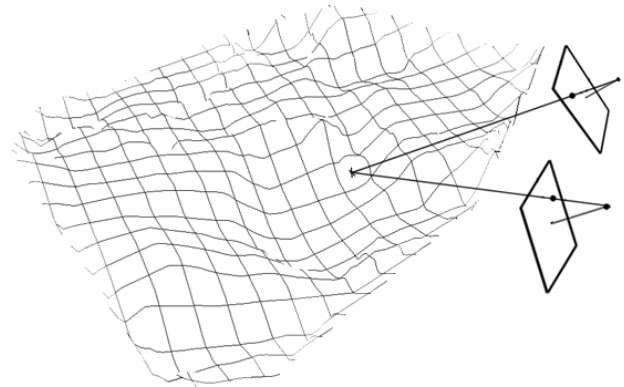


Figure 1. Rays traversing from the focal centres are constrained to intersect on the planar surface patch.

### 2.1 Homologous points extraction

For the identification of homologous points the Scale-Invariant-Feature-Transform (SIFT) (Lowe, 2004) is used. The SIFT is a methodology for finding corresponding points in a set of images. The method designed to be invariant to scale, rotation, and illumination. The methodology consists of: i) detection of candidate interest points via scale-space extrema search, ii) localization of the keypoints, iii) orientation assignment based on the image local gradient to ensure scale and orientation invariance, and iv) descriptor computation. For each detected keypoint a descriptor which is invariant to scale, rotation and changes in illumination, is generated. The descriptor is based on orientation histograms in the appropriate scale. Each descriptor consists of 128 values.

The extraction of candidate counterpart points is vital in the present case for two purposes: the first is the establishment of the relative orientation between image pairs, and the second is launching the point-to-surface registration model. These two goals have two different objectives, the first is obtaining a reliable set of points for orientation where the focus is on their quality, and the second is obtaining a detailed surface model, with focus on quality but also on their quantity. In this regards, the ability to control the amount of keypoints extracted by the SIFT model provides an excellent and efficient means for the provision of large set of potential 3D points. Therefore, the counterpart extraction process is applied here in two parts.

For the relative orientation, a high filtering threshold is set, so that only a marginal number of outliers result. Considering the fact that for the computation of the relative orientation only five points are required, setting a high threshold still provides a great number of degrees of freedom than what is customary to use.

The computed relative orientation also defines the geometrical locus where all candidate counterparts of a given point can be found. Therefore, for second phase that concerns describing the surface, the initial filtering threshold value for potential corresponding points is decreased. Matches are not only evaluated by their descriptor similarity, but also by their proximity to the epipolar line in the second image. Proximity is computed by the image distance between a point and the epipolar line it is expected to lie on. Points whose distances exceed a certain threshold value are discarded. The distance is a function of the accuracy of the estimation of the relative orientation. Notice that outlying matches that lie along epipolar lines cannot be detected. However, as the following show, they are easily detected by using the absolute orientation phase.

## 2.2 Absolute orientation model

With the establishment of a relative orientation between the two images, the computation of the absolute orientation is next step to follow. For that, the photogrammetric data is given by a set of autonomously derived corresponding points and control information given by a surface model. The goal is to determine the best estimation of the similarity transformation between the photogrammetric and the control datasets. The underlying assumption in the determination of similarity transformation is that both datasets represent the same object, and that the differences between them are in the form of translation, rotation, and scale. In the present case, this translates into the assumption that both the photogrammetric pointset and the control surface are samples of the real-world topography. We define the similarity transformation from the photogrammetric model coordinate system to the control coordinate system by

$$\mathbf{p} = m \cdot \mathbf{R} \cdot (\mathbf{p}' - \mathbf{t}) \quad (1)$$

with  $\mathbf{p}'$  a point in the photogrammetric model system,  $\mathbf{p}$  a point in the control coordinate system,  $\mathbf{t}$  the translation between the two systems,  $\mathbf{R}$  the orthonormal rotation matrix, and  $m$  the scale factor.

Registration between 3D datasets falls within the class of iterative closest point (ICP) procedures on all their variants. Besl and McKay (1992) propose identifying point-pairs autonomously, and with the proposed correspondence between point-pairs compute a rigid-body transformation. Convergence is reached when the actual matches are found. Estimating the transformation vector when no true correspondence between the sets exists, leads to a biased estimation. The magnitude of the bias will depend on “how far” the sets are from establishing a true correspondence. For practical purposes, when at least one pointset is extremely dense (e.g., points cloud generated using laser scanners), it can be assumed that such correspondence exists. Such setup leads to a negligible bias, which is far smaller than the variances associated with the estimation. Chen and Medioni (1992) introduce point-to-surface registration for determining the rigid body transformation. Parameters are based on minimizing the sum of square-distances between a pointset and a surface. Grün and Akca (2005) also add a scale factor into the algorithm.

The common surface models are usually provided either in the form of a regular-grid or by a set of irregularly distributed points. For the latter case the triangular-irregular-network (TIN) is usually established as a surface representation. Regular grids are easy to generate, manipulate, and access, however they are limited to 2.5D and by nature limited to work with regular data. The TIN representation is more general than the regular grid

model, more flexible, and can be employed to a full 3D model as well. The common use of TIN representation and its greater flexibility motivate the formulation of the solution with this representation.

The local surface patches in the TIN, defined by the three triangle vertices, are considered planar. The point-to-plane distance  $\delta_i$  can then be written in vector form is

$$\delta_i = \begin{bmatrix} \mathbf{n}_i^T & d_i \end{bmatrix} \cdot \begin{bmatrix} \mathbf{p}_i \\ 1 \end{bmatrix} \quad (2)$$

with  $\mathbf{n}_i = [n_i^x, n_i^y, n_i^z]^T$  the normalized (unit length) normal vector to the plane defined by triangle  $t_i$ ,  $d_i$  the plane constant, and  $\mathbf{p}_i = [x_i, y_i, z_i]$ . Linking Eq. (1) and Eq. (2) leads to

$$-m\mathbf{n}_i^T \mathbf{R} \mathbf{t} + m\mathbf{n}_i^T \mathbf{R} \mathbf{p}'_i + d_i - \delta_i = 0 \quad (3)$$

The origin of both coordinate systems – the photogrammetric and the control ones, are transformed to their respective centroids. The quantities in Eq. (3) can be categorized as belonging into observations and unknowns.  $\mathbf{p}'_i$ ,  $\mathbf{n}_i$  and  $d_i$  are the observations and  $\mathbf{s} = [t_x, t_y, t_z, m, \dots]^T$  is the vector of unknown transformation parameters. We would like to prevent deformations to the control surface during the adjustment process thus considering  $\mathbf{n}_i$  and  $d_i$  as constants. Eq. (3) is non-linear, so in order to perform a least-squares estimation, linearization using Taylor series expansion leads to

$$\mathbf{A} \mathbf{s} + \mathbf{B} \mathbf{v}_p - \mathbf{v}_\delta + \mathbf{w} = 0 \quad (4)$$

with  $\mathbf{s}$  the differential correction to the initial transformation parameters approximations,  $\mathbf{v}_p$  and  $\mathbf{v}_\delta$  the residuals of the point and distance observations respectively, and

$$\mathbf{A} = \frac{\partial f(\mathbf{S}, \mathbf{p}, T)}{\partial \mathbf{S}}; \quad \mathbf{B}_p = \frac{\partial f(\mathbf{S}, \mathbf{p}, T)}{\partial \mathbf{p}}$$

$a_i$  and  $b_{i,j}$ , the respective rows of  $\mathbf{A}$  and  $\mathbf{B}$  corresponding to the condition equation written for the  $i^{\text{th}}$  point are given in Eq. (9)

with  $r_{ij}$  the value in row  $i$  and column  $j$  of  $\mathbf{R}$  and  $\overline{\mathbf{p}}_i^B = \mathbf{p}_i^B - \mathbf{t}$ .

The least-squares target function becomes then

$$\mathbf{s}^T \mathbf{P}_s \mathbf{s} + \mathbf{v}_p^T \mathbf{P}_p \mathbf{v}_p + \mathbf{v}_\delta^T \mathbf{P}_\delta \mathbf{v}_\delta - 2\mathbf{k}^T (\mathbf{A} \mathbf{s} + \mathbf{B} \mathbf{v}_p - \mathbf{v}_\delta + \mathbf{w}) = \min \quad (5)$$

with  $\mathbf{P}_p$  and  $\mathbf{P}_\delta$  the weight matrices for the observations,  $\mathbf{P}_s$  the weight matrix for the initial values of the unknowns, and  $\mathbf{k}$  the vector of Lagrange multipliers. Solving Eq. (5) leads to

$$\hat{\mathbf{s}} = -\mathbf{N}^{-1} \mathbf{A}^T \mathbf{M}^{-1} \mathbf{w} \quad (6)$$

$$\hat{\mathbf{v}}_p = -\mathbf{P}_p^{-1} \mathbf{B}_p \mathbf{M}^{-1} (\mathbf{A} \hat{\mathbf{s}} + \mathbf{w}) \quad (7)$$

$$\hat{\mathbf{v}}_\delta = -\mathbf{P}_\delta^{-1} \mathbf{B}_\delta \mathbf{M}^{-1} (\mathbf{A} \hat{\mathbf{s}} + \mathbf{w}) \quad (8)$$

with  $\mathbf{N} = \mathbf{A}^T \mathbf{M}^{-1} \mathbf{A} + \mathbf{P}_s$  and  $\mathbf{M} = \mathbf{B}_p \mathbf{P}_p^{-1} \mathbf{B}_p^T + \mathbf{P}_\delta^{-1}$

The a posteriori variance is given by

$$\mathbf{a}_i = \begin{bmatrix} t_x & t_y & t_z & m & \omega & \phi & \kappa \\ -m\mathbf{n}_i^T \begin{bmatrix} r_{11} \\ r_{21} \\ r_{31} \end{bmatrix} & -m\mathbf{n}_i^T \begin{bmatrix} r_{12} \\ r_{22} \\ r_{32} \end{bmatrix} & -m\mathbf{n}_i^T \begin{bmatrix} r_{13} \\ r_{23} \\ r_{33} \end{bmatrix} & \mathbf{n}_i^T \mathbf{R} \bar{\mathbf{p}}_i^B & m \cdot \mathbf{n}_i^T \cdot \frac{\partial \mathbf{R}}{\partial \omega} \cdot \bar{\mathbf{p}}_i^B & m \cdot \mathbf{n}_i^T \cdot \frac{\partial \mathbf{R}}{\partial \phi} \cdot \bar{\mathbf{p}}_i^B & m \cdot \mathbf{n}_i^T \cdot \frac{\partial \mathbf{R}}{\partial \kappa} \cdot \bar{\mathbf{p}}_i^B \end{bmatrix} \quad (9)$$

$$\mathbf{b}_{p_i} = \begin{bmatrix} x_1 & y_1 & z_1 & \dots & x_i & y_i & z_i & \dots & x_n & y_n & z_n \\ 0 & 0 & 0 & \dots & m \cdot \mathbf{n}_i^T \cdot \begin{bmatrix} r_{11} \\ r_{21} \\ r_{31} \end{bmatrix} & m \cdot \mathbf{n}_i^T \cdot \begin{bmatrix} r_{12} \\ r_{22} \\ r_{32} \end{bmatrix} & m \cdot \mathbf{n}_i^T \cdot \begin{bmatrix} r_{13} \\ r_{23} \\ r_{33} \end{bmatrix} & \dots & 0 & 0 & 0 \end{bmatrix}$$

$$\hat{\sigma}_0^2 = \frac{\hat{\mathbf{S}}\mathbf{P}_s\hat{\mathbf{S}}^T + \hat{\mathbf{v}}_p\mathbf{P}_p\hat{\mathbf{v}}_p^T + \hat{\mathbf{v}}_\delta\mathbf{P}_\delta\hat{\mathbf{v}}_\delta^T}{n - u} \quad (10)$$

with  $n$  the number of condition equations (equals to the number photogrammetric model points), and  $u$  the number of transformation parameters (seven here). The covariance matrix of the estimated parameters will be

$$\Sigma_s = \hat{\sigma}_0^2 \cdot \mathbf{Q}_s \quad (11)$$

with  $\mathbf{Q}_s$  the cofactor matrix given by  $\mathbf{Q}_s = \mathbf{N}^{-1}$ . Since the control surface is the best knowledge we have regarding the topography, the value of  $\hat{\sigma}_0^2$  is set to zero. The same reasoning leads to assigning large weights to  $\mathbf{P}$  the weight matrix of the independent variable. An advantage of the proposed model is that if one of the entities has the potential of being erroneous (meaning unreliable control surface is at either the specific point or outlying point coordinates) its corresponding weight can be reduced and easily discarded from the solution. Furthermore, when  $\mathbf{P} \rightarrow 0$  virtually becomes unknown, its residual values  $\hat{\mathbf{v}}$  provide an indication to the quality of the constraint. It should be noted that setting moderate values to the weight matrix of  $\hat{\mathbf{v}}$ ,  $\mathbf{P}$ , (i.e., close to the values of  $\mathbf{P}_p$ , the pointset weights) leads to high correlation between  $\hat{\mathbf{v}}$  and  $\hat{\mathbf{v}}_p$ .

The discrete, piecewise, representation of the surface by the TIN model requires establishing correspondence between the points and the triangles. The model defines that a point is related to a triangle if: i) the point is inside the triangle – a vector from the point to the triangle, with direction parallel to the normal to the triangle plane, intersect the triangle plane inside of it, and ii) the distance between the point and the triangle plane is the minimum with respect to all triangles that answer condition (i). A threshold value is set such that points that are too far from the surface will not be associated to any triangle, thus minimizing the effect of outliers.

### 2.3 Quality of the solution

An analyzing the quality and stability of the surface-based solution is studied by analyzing the trace of the dispersion matrix, the condition number, and correlations between the estimated parameters. The analysis shows that quality of the parameter estimation increases when surface normals have large variability, namely when they are well distributed in all directions. Accuracy estimates for the translation parameters increases as a function of the sum of squared surface normals in

their respective directions. The scale factor accuracy increases as more surface normals are pointing to the centroids of the pointset, and rotations accuracy increases with the sum of normals orthogonal to their respective axes.

Testing the model in various simulated and real world setups shows condition number of 100-1000, average correlation coefficient of 0.2-0.4 and under adequate representation the redundancy number is 0.7-0.9. These indicate a uniform quality of the solution, parameter dependency, and ease of tracing gross observation errors.

Prior to turning to the presentation of the results, we note that even though not detailed here, a model for surface-based bundle adjustment can be applied by adding to the collinearity observations a point-on-surface constraint. The surface-based bundle adjustment model can be found in Levin (2008).

## 3. RESULTS AND DISCUSSION

The application of the proposed model is demonstrated on a documentation project in the Rakefet cave, an archeological excavation site in the Carmel mountain ridge, as part of an ongoing research studying the origins and use of Manmade-bedrock-holes in those sites. Two mapping campaigns have been performed in the small area of ~60 m2, among the two one was photogrammetric based. As an archeological site, no permanent markers could have been placed in the site to serve as control network. An existing terrain-model (see figure 2), which coarsely represents the surface in some parts, is used as control information. The terrain model contains about 2900 point and about 4600 triangles. Images were acquired with a Nikon D70 camera, with 28 mm Nikkor lens.

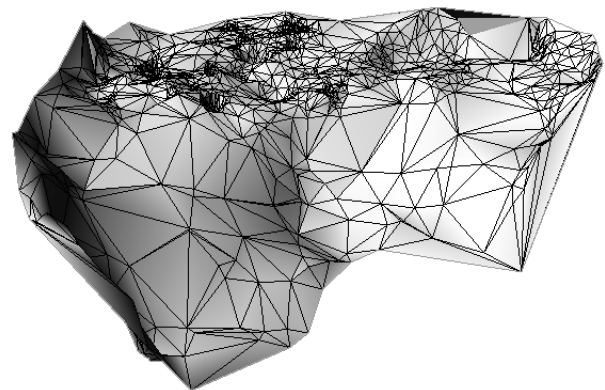


Figure 2. Control surface for Rakefet cave.

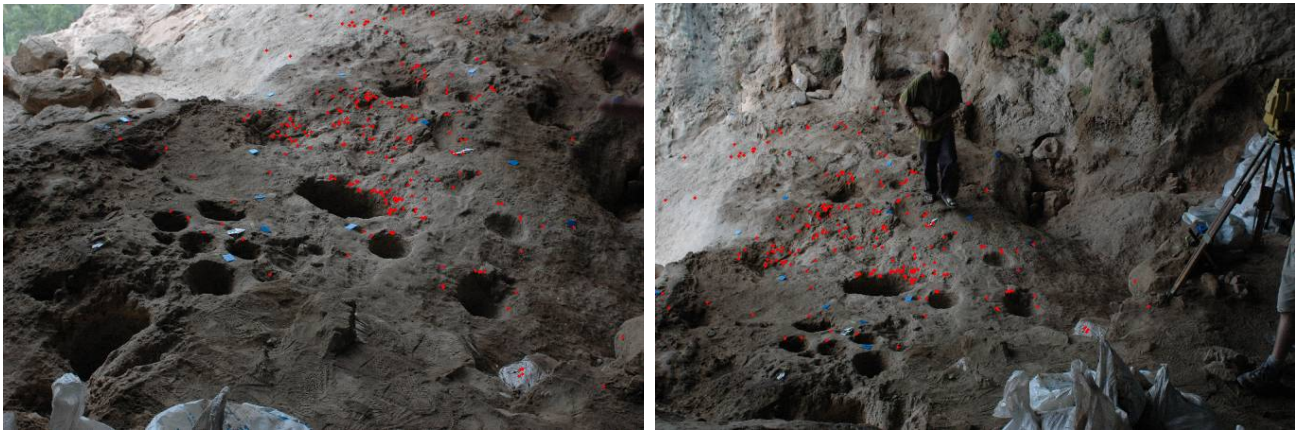


Figure 3. Images of the cave floor. SIFT matched homologous points indicated by red points.

Applying the SIFT algorithm on the image set resulted in a set of 262 points that were autonomously extracted. Among them 31 points have passed the high threshold filtering stage (threshold was set to 6) and the rest were found corresponding by limiting the search to the epipolar line locus. Of the 31 points that were used for the relative orientation phase none were outlying. Similar results were observed in other stereopairs on which the keypoint extraction model was applied. The set of homologous points are presented in figure 3, while being marked on the images. The mean depth for a point in the model system was three base lengths, and the mean estimated standard deviation is 1.2% of a base length. The based length itself was 100 units.

For initial approximation of the orientation parameters, a user-interactive correspondence finding scheme was applied. Approximation for a surface-based photogrammetric scheme requires matching two model points to surface entities. The first point allows defining the orientation by matching normals (up to one degree of freedom), and the translation vector. The second point solves the remaining degree of freedom in the orientation assignment, and the scale factor.

The approximated scale factor was 0.018, resulting in an expected point accuracy of  $1.2 \cdot 0.018 = 0.02m$ . Based on the expected accuracy, the threshold for association of point to triangle was defined as 0.20m. The estimation of parameter accuracy and model quality are presented at table 1. An overlay of the reconstructed surface on the original topographic model is shown in figure 4.

|  | $t_x$ [m] | $t_y$ [m] | $t_z$ [m] | $m$  | $\sigma_x$ [°] | $\sigma_y$ [°] | $\sigma_z$ [°] |
|--|-----------|-----------|-----------|------|----------------|----------------|----------------|
|  | 0.02      | 0.01      | 0.01      | 0.01 | 0.2            | 0.3            | 0.5            |
| $\hat{\sigma}_0 = 0.03m; \quad tr(\Sigma_s) = 0.001; \quad c_{\#} = 133; \quad  \bar{\rho}  = 0.3$ |           |           |           |      |                |                |                |

Table 1. Estimation of the parameter accuracy, and measurements of model robustness, for the absolute orientation of the Rakefet cave model.

It can be seen that the estimated translation accuracies are, as expected, at the order of magnitude of  $\sigma_0$ , which is quite close to the approximated accuracy for a model point of 0.02m. The condition number indicates a uniform solution and the average correlation coefficient is low, indicating high parameter independency. Redundancy numbers were computed for the

observations, yielding mean planar redundancy number  $r_{xy}=0.1$ , and vertical redundancy number  $r_z = 0.8$  indicating that vertical observation error will be easily detected.

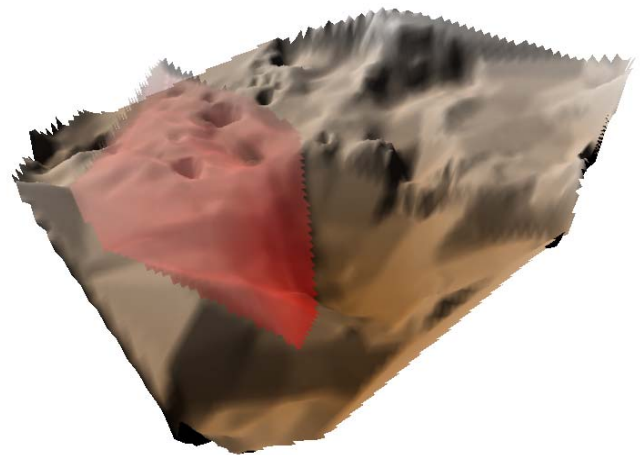


Figure 4. Results for the absolute orientation process for Rakefet cave. It is clearly visible that the photogrammetric data (red surface) fits well the control surface (brown surface).

To better assess the differences between the control surface and the photogrammetric pointset, the distances of the geo-referenced points from the control surface was computed and arranged in the histogram shown in figure 5.

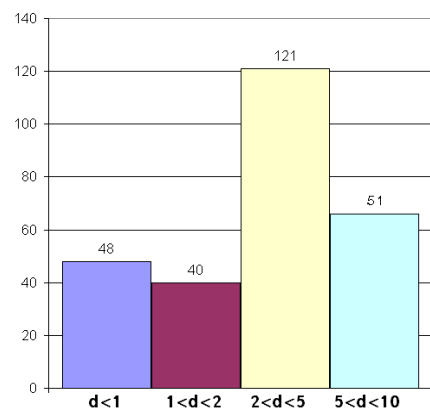


Figure 5. Distances of the geo-referenced pointset from the control surface.

At first impression, the histogram may appear surprising, as the majority of points lie in a distance of 2–5 cm from the surface, while the condition equation constrained the point to lie on the surface. However, the absolute orientation is a similarity transformation, allowing translation, rotation and scale difference but meaning that the shape of the dataset cannot be deformed. The bin containing most of the points is also the bin corresponding to the expected accuracy of a measurement with unit weight. Accounting for random error in the observations and control surface, these results reflect the natural surface roughness of the floor cave. In this regards the majority of the points can be considered as added detail to the surface.

#### 4. CONCLUSIONS

This paper has demonstrated the utilization of surface-data as control entity. It has shown how surfaces allow for fast and accurate geo-referencing of close-range photogrammetric blocks while relieving the need for establishing control point network, and identifying those in the image set. Such models are useful for the documentation of archeological and heritage sites, which are often complex and cannot be easily accessed.

It has been shown that establishing a set of reference entities from the photogrammetric images is fast using the SIFT model. A set of nearly 300 points can usually be derived from the image pairs under reasonable imaging conditions. The manual correspondence assignment is relatively simple to establish, and is far simpler than the point based one.

Although formulated for use with TIN surface representation, the model is based on surface normals and distances from the surfaces, thus applies for any type of surfaces.

#### REFERENCES

- Besl, P. and McKay, N. 1992. A Method for Registration of 3-D Shapes. Trans. on *PAMI*, **14**(2), 239 - 256.
- Chen, Y., Medioni, G., 1992. Object modeling by registration of multiple range images. *Image and Vision Computing* **10** (3), 145–155.
- Ebner H, Strunz G. and Colomina I, 1991. Block Triangulation with Aerial and Space Imagery Using DTM as Control Information. *International Archive of Photogrammetry and Remote Sensing* **27**(B11), pp. III/578-587.
- Ebner H. and Ohlhof T, 1994. Utilization of Ground Control Points for Image Orientation Without Point Identification In Image Space.
- Eisenbeiss H., Lambers K., Sauerbier M., Zhang L. (2005). Photogrammetric documentation of an archaeological site (palpa, peru) using an autonomous model helicopter. CIPA 2005 XX International Symposium WG I.
- El-Hakim, S., Gonzo, I., Voltolini, F., Girardi, S., Rizz, A., Remondino, F., Whiting, E., 2007, Detailed 3D Modeling of Castles. *International Journal of Architectural Computing*. **5**(2). 199-220.
- Grün A. and D. Akca, 2005. Least squares 3D surface and curve matching. *ISPRS Journal of Photogrammetry & Remote Sensing* **59**(3), 151–174.
- Habib, A. F., M. S. Ghanma and M Tait, 2003. Integration of Lidar and Photogrammetry for Close Range Application. PS, WG I/5, Platform and Sensor Integration.
- Hartley, R. and Zisserman, A., 2004. *Multiple View Geometry in Computer Vision*. Cambridge University Press.
- van den Huvel, F., 1999. Line photogrammetry mathematical model for the reconstruction of polyhedral objects. in proceeding of *SPIE* vol. 3641: 60-71.
- Jaw, J.J., 2000. Control Surface In Aerial Triangulation. *International Archives of Photogrammetry and Remote Sensing*. **33**(3B). Amsterdam.
- Kulur, S. F. Yilmaztürk, 2005, 3D-reconstruction of small historical objects to exhibit in virtual museum by means of digital photogrammetry, CIPA 2005 XX International Symposium WG I
- Lazaridou, M. , E. Patmios, 2005. PHOTOGRAMMETRY AND image interpretation on the study of architectural and natural cultural eritage. CIPA 2005 XX International Symposium WG I
- Lerma, J. L., Villaverde V., García A., Cardona J., 2005, close range photogrammetry and enhanced recording of palaeolithic rock art, *IAPRS* **36**(5), Dresden 25-27 September 2006
- Levin, S., 2008. Close-Range Photogrammetry using DTM as Control Surfaces. MSc thesis, Faculty of Civil and Environmental Engineering, Technion – Israel Institute of Technology, Haifa, Israel, 107 p.
- Lowe, D.G. 2004. Distinctive Image Features from Scale-Invariant Keypoints.
- Schenk T., 2004. From point-based to feature-based aerial triangulation. *ISPRS Journal of Photogrammetry & Remote Sensing* **58**, 315– 329.
- Zalmanson, G., 2000. Hierarchical Recovery of Exterior Orientation from Parametric and Natural 3D Curves. PhD dissertation. Department of Civil and Environmental Engineering and Geodetic Science, The Ohio State University, Columbus, OH 43210. 121 pp.